



SPE 71326

# Saturation Height Methods and Their Impact on Volumetric Hydrocarbon in Place Estimates

B. Harrison (Enterprise Oil) and X.D. Jing (Imperial College, London)

Copyright 2001, Society of Petroleum Engineers Inc.

This paper was prepared for presentation at the 2001 SPE Annual Technical Conference and Exhibition held in New Orleans, Louisiana, 30 September–3 October 2001.

This paper was selected for presentation by an SPE Program Committee following review of information contained in an abstract submitted by the author(s). Contents of the paper, as presented, have not been reviewed by the Society of Petroleum Engineers and are subject to correction by the author(s). The material, as presented, does not necessarily reflect any position of the Society of Petroleum Engineers, its officers, or members. Papers presented at SPE meetings are subject to publication review by Editorial Committees of the Society of Petroleum Engineers. Electronic reproduction, distribution, or storage of any part of this paper for commercial purposes without the written consent of the Society of Petroleum Engineers is prohibited. Permission to reproduce in print is restricted to an abstract of not more than 300 words; illustrations may not be copied. The abstract must contain conspicuous acknowledgment of where and by whom the paper was presented. Write Librarian, SPE, P.O. Box 833836, Richardson, TX 75083-3836, U.S.A., fax 01-972-952-9435.

## Abstract

The paper reviews four of the more popular saturation-height methods employed in the oil and gas industry, namely those proposed by Leverett, Johnson, Cuddy and Skelt. The advantages and drawbacks of each method are highlighted. Each technique is compared by investigating how accurately they model the saturation-height profiles of a Palaeocene oil well from the UK Central Graben and a Permian gas well from the UK Southern North Sea. Both wells have complete data sets including conventional core, SCAL and a comprehensive suite of electric logs. Besides comparing each of the methods on a well basis, the paper applies the resultant saturation-height relationships to the reservoir structures to see the effect on the computed hydrocarbon-in-place estimates. By moving to an areal field-wide basis, the effects of reservoir structural relief and the relative importance of the transition zone modelling is brought into focus.

## Introduction

A former colleague of ours once stated that petrophysicists only produce three numbers of any interest to others, namely, porosity, saturation and net to gross. While there may be a grain of truth in his cynicism, he forgot to mention that one other major deliverable of petrophysics, the saturation-height function. Armed with this algorithm, the geologist or reservoir engineer is able to predict the saturation anywhere in the reservoir for a given height above the free water level and for a given reservoir permeability or porosity, or to estimate permeability once water saturation is known. So far, so good, but the fly in the ointment is that there are many saturation-height methods to choose from. Which method should one use? Does it really matter?

To investigate these questions, we applied four of the more commonly used saturation-height routines to two complete data sets from wells in the North Sea; one oil well and one gas well. Each of the subsequent predictive equations was then integrated with a gross rock area vs. depth curve in order to compute the in place hydrocarbon volumes for each reservoir. Based on the results, we then attempted (maybe foolishly, given how stubbornly some analysts defend their favourite methods) to recommend which approach should be used for particular circumstances. You will see that (as usual in petrophysical and indeed any subsurface geoscience and reservoir engineering matters) the outcome is not cut and dried.

## Background Theory<sup>(1,2)</sup>

Capillary pressure reflects the interaction of rock and fluids, and is controlled by the pore geometry, interfacial tension and wettability. The capillary pressure concept is an important parameter in volumetric studies where it is used to calculate fieldwide saturation-height relationships from core and log information. It is also employed to infer the free water level (FWL) from oil transition zone saturation-height relation when valid pressure gradient data for both oil and water legs may not be available. Once a fieldwide saturation-height transform has been created as a function of permeability, it can be inverted to predict permeability in uncored regions of the field. The relationship is especially useful when drilling infill wells later in field life and it is found that zones have been partially swept. Hence, the infill well saturations will not reflect initial conditions, but the saturation-height relation can be used instead. The relation can thus be used to estimate the extent of flushing of the producing zones and so give an estimate of sweep efficiency.

We can see how capillary pressure relates to the rock and the fluids therein by reviewing the Young-Laplace equation for an immiscible fluid pair in a circular cross-section pore at lab conditions:

$$P_c = \frac{2\sigma \cos \theta}{r} \dots\dots\dots(1)$$

where  $\sigma$  is the interfacial tension (a fluid property);  $\theta$  is the contact angle (related to wettability and rock-fluid interaction)

and  $r$  is the pore radius (rock property related to permeability and porosity). The laboratory values of capillary pressure must be converted to equivalent reservoir condition values as follows:

$$P_c(res) = P_c(lab) \frac{(\sigma \cos\theta)_{res}}{(\sigma \cos\theta)_{lab}} \dots\dots\dots(2)$$

Typical values for interfacial tension and contact angles are taken from the Corelab manual <sup>(3)</sup> and are given in Table 1. There are other good sources of these values available and interfacial tension (IFT) can be measured under reservoir conditions of pressure and temperature <sup>(4)</sup>.

The lab-to-reservoir conversion, however, only considers the difference in capillary pressure due to interfacial tension and contact angle and ignores other measurement conditions. Interfacial tension can be measured at laboratory and reservoir conditions, but the contact angle is difficult to quantify (especially for systems that are not strongly wet, i.e. most oil reservoirs). Therefore, in practice other than dry gas reservoirs, the above conversion needs to be calibrated against in-situ saturation-height above FWL where the saturation data need to be derived from logs or oil-based cores. Its common to observe a higher capillary transition zone derived from core based drainage capillary pressure curves (air/brine or air/Hg) than that derived from resistivity logs. Assuming the log-derived saturation is reliable, one main reason for any disparity may be due to the above conversion from laboratory to reservoir conditions failing to take into account reservoir interfacial tension, stress effects and, more likely, wettability.

#### Converting Capillary Pressures to the Height Domain.

The pressure gradients for the oil and water phases are determined by the fluid densities. The water saturation distribution above FWL (or below FWL for a negative capillary pressure in an oil-wet system) is controlled by the balance of capillary and buoyancy (gravity and density difference) forces:

$$P_c = (\rho_w - \rho_o)gh \dots\dots\dots(3)$$

In oilfield units where  $P$  is in psi,  $h$  is in feet relative to the FWL and fluid densities are in  $\text{lbm/ft}^3$ :

$$P_c = \frac{h(\rho_w - \rho_o)}{144} \dots\dots\dots(4)$$

Some analysts prefer to use the pressure gradients of each phase in psi/ft as these relate better to the wireline formation tester data:

$$P_c = h (\text{water gradient} - \text{oil gradient}) \dots\dots\dots(5)$$

Remember that when using wireline formation tester data, we traditionally treat the intersection of the gas and oil pressure

gradients as the free oil level (FOL), not the gas oil contact (GOC). Likewise, we treat the intersection of the oil and water pressure gradients as the FWL, not the oil water contact (OWC).

**Characteristics of Capillary Pressure Curves.** Reservoir water saturation decreases with increasing height above the FWL, where capillary pressure is zero. A minimum water saturation ( $S_{wirr}$ ) is reached at a great height above the FWL and this water saturation is immobile. The transition zone is defined as the zone which can produce both hydrocarbon and water. Variations in the capillary radius are controlled by the pore geometry, which is a function of rock properties such as permeability and porosity. Hence, pore size distribution has a major influence on the magnitude of the irreducible water saturation and the extent and height of the transition zone. The hydrocarbon water contact (HWC) will vary with depth as a function of the reservoir quality, i.e. the higher the permeability, the smaller the separation between the OWC and the FWL. The GOC also varies in depth, in proportion to the interfacial tension difference between the gaseous and liquid hydrocarbon, but the variation is much less than that of the OWC due to the higher density difference between gas and liquid.

#### Reconciliation with Other Data

Whichever saturation-height function is used to derive fieldwide saturation distribution, it is always important to check the calculated water saturation values against other independent data sources.

For example, we routinely cross check the results of our saturation-height function against log derived water saturation values. However, it is necessary to note the limitations of log measurements and their interpretation. A common problem with conventional electrical logs is poor resolution in thinly bedded formations (laminations occur within less than 1m interval). Other problems include the effects of the mud filtrate invasion, water imbibition processes, clay excess conductivity and determination of the Archie saturation exponent “ $n$ ” that is itself wettability dependent during imbibition.

We also compare the results of a saturation-height function with the values of water saturation extraction from cores cored with oil based mud (OBM). Direct water saturation from Dean-Stark extraction of OBM cores after formation volume factor correction is another source of saturation data. Unfortunately, this data is usually limited due to the requirement of good core coverage. We were fortunate to have Dean-Stark water saturation data in our oil well example and it showed that the log derived water saturation above the transition zone was reasonable. In fact, the SCAL capillary pressure derived water saturation seemed to be at fault, seemingly the plugs weren’t de-saturated to irreducible water saturation and capillary pressure equilibrium may not have been reached.

For reservoirs with large areal extent and low relief, the transition zone will have a significant impact on the

hydrocarbon volume. Independent water saturation measurements from wells penetrating the transition zone and covering a range of reservoir qualities are recommended to constrain and calibrate the water saturation calculations from core capillary pressure based saturation-height functions.

The field pressure data is another valuable source of information to locate FWL and constrain saturation-height functions. There is also often ambiguity if a well does not penetrate both the oil and water legs to allow sufficient pressure points to be taken to define the phase pressure lines and interception. Regional water pressure lines may have to be used. The effect of OBM invasion-induced capillary pressure in water legs, particularly for tight water-wet reservoirs, can lead to the measured FWL to be significantly higher than the true FWL. Also beware of supercharging, which causes scattering of pressure data points.

**Saturation-Height Equations**

There are various practical techniques for correlating capillary pressure curves according to rock type for a heterogeneous formation and generating field wide saturation-height function that relates capillary pressure curves to porosity, permeability or rock type in general. The classic method is based on Leverett’s J-function approach <sup>5</sup>. Other commonly used methods in the UKCS include Johnson <sup>6</sup>, Cuddy et al. <sup>7</sup> and Skelt-Harrison <sup>8,9</sup>. Although developed using UK field data, their use is not restricted to the North Sea. For instance, we have seen the Skelt-Harrison technique applied with success in Venezuela and Indonesia. This paper presents a brief description of these methods and a comparative study of the performance of the selected saturation-height methods in estimating field saturation distribution and the subsequent impact on STOIP estimates based on two field examples from the North Sea, UKCS. The examples are based on drainage capillary pressure curves. The same procedure can be applied to imbibition or oil-wet/mixed-wet field cases subject to a thorough understanding of the reservoir processes and availability of relevant field and core data.

**Capillary Pressure-based Method 1 (Leverett<sup>5</sup>).** We can see from equation (1) that the parameter group  $(P_c.r)/(\sigma.\cos \theta)$  is dimensionless. As permeability has the units of area, we could substitute the square root of permeability for the mean pore radius “r” and still retain the dimensionless nature of the group. Leverett proposed just such a dimensionless capillary pressure group, and he derived the term  $(K/\phi)^{0.5}$  instead from a simple pore-space model. This term is the pore geometry factor with the same dimension as pore radius "r" and is used for correlating petrophysical properties including relative permeability and residual saturations. Leverett’s subsequent “J-function” attempts to convert all capillary pressure data, as a function of water saturation, to a universal curve:

$$J(S_w) = \frac{P_c}{\sigma \cos \theta} \sqrt{\frac{K}{\phi}} \dots\dots\dots(6)$$

The “cos θ” term was added later to adjust for wettability. Special core analysis (SCAL) measurements of capillary pressure on core samples provide the most reliable means to establish J-functions for rock types with similar pore geometries. Capillary pressure measurements are performed on each core plug and, after conversion to reservoir conditions, are then converted to J values for each sample and plotted against saturation. For a set of samples with similar pore size distributions, a least squares regression analysis is then made using the J values as the independent variable. The best correlation is often obtained using a power law equation of the form:

$$J = a (S_w)^b \dots\dots\dots(7)$$

The J-function has been widely used as a correlating group for all capillary pressure measurements using different fluid systems, but it **only applies** if the porous rock types have similar pore size distributions or pore geometry. In these types of rocks, the pore size and permeability increase as the grain size increases. If a rock contains a significant amount of micro-porosity in the very small pore spaces, water saturation in the above equation may be replaced by  $(S_w - Sw_{irr})$ . Best results are usually found when data for given formations and rock types are correlated separately. A lack of correlation suggests the need of further zonation. Once a J-function has been established for each rock type, they can be used in the field to relate saturation with height above FWL, permeability and porosity. The averaging nature of the Leverett J-function means it gives poorer results if the dynamic range of permeability is large, say several orders of magnitude. It seems to perform best when the range of permeability is only within 2-3 orders of magnitude.

**Capillary Pressure-based Method 2 (Johnson<sup>6</sup>).** Another way of correlating capillary pressure data uses the observation that, for a given rock type, capillary pressure measurements on core samples of different permeabilities form a family of curves. Taking this lead, Johnson proposes relating mathematically the water saturation from capillary pressure measurements to permeability. Approximate linearisation is achieved by plotting the variables on log/log axes. Using SCAL data, Johnson observed that the plots of water saturation vs. permeability for each capillary pressure de-saturation step were approximate straight and parallel lines when drawn on log/log axes. His “permeability averaging” method gives an empirical function, shown below, that relates capillary pressure (or height above FWL) to water saturation and permeability.

$$\log (S_w) = B . P_c^{-C} - A . \log (K) \dots\dots\dots(8)$$

Parameters A, B and C are constants, Sw is in percent, k is in mD and Pc is in psi. Constants A, B and C are derived from SCAL capillary pressure data using a series of crossplots. These are time consuming to construct and it is our experience

that the Johnson method is one of the more labour intensive if the crossplots technique is adopted. Non-linear regression analysis is suggested to derive the parameters. For small capillary pressure values, i.e. a short distance above the FWL, the equation tends to blow up (predicted water saturation > 1) and needs to be clipped. The paper uses the Argyll field from the Central North Sea as an example of the method. This oil field has a Permian age, Rotliegendes reservoir comprised of good quality massive aeolian dune sands with high primary porosity (12-28%) and high net to gross. Permeability ranges from 10-1000 mD and connate water saturation ranges from 20 - 50%. In the paper, the computed conversion factor of capillary pressure from lab-to-reservoir using equation (2) was a factor of seven lower than the theoretical textbook value when matched to log-derived water saturation data in the Argyll field. Johnson states that his method is not universal, but it has proved effective in some North Sea reservoirs.

**Log-based Method (Cuddy et al.<sup>(7)</sup>).** Cuddy et al. postulates that the product of porosity and saturation can be a function of height alone. In many of the gas reservoirs in the Southern North Sea, one observes a self compensating system between porosity and water saturation, above the transition zone, as porosity increases, so water saturation decreases, and vice versa. Hence, the Bulk Volume Water (BVW), which is the product of porosity and water saturation, is effectively a constant above the transition zone. Cuddy et al. uses log-derived water saturation values only to derive the function, choosing to ignore SCAL based capillary pressure measurements. Thus, Cuddy et al. plots BVW vs. height above FWL on log-log scale and the equation has the form:

$$\log(\phi \cdot S_w) = A \cdot \log(h) + B \dots\dots\dots(9)$$

where h is height above FWL and A and B are constants found by regression. Cuddy et al. claims that their technique is virtually independent of permeability and porosity. They state that other saturation-height methods are simply fits to data and are not based on rock physics, unlike their method. Some analysts dispute this claim. In the original paper, Cuddy et al. used the equation in a curve-fitting algorithm to find the FWL. This may not be good practice as the problem is poorly conditioned and the accuracy of the data is inherently low. The method takes no account of lithology and is biased towards fitting the water saturation data in the better quality sands. Only net reservoir data, that is more than 1m from a bed boundary (to eliminate data that is affected by different vertical logging tool responses), is used for line fitting. This may produce incorrect water saturation values within the lower porosity intervals. However, the technique is much simpler and much easier to develop than the other methods outlined in this paper. It also requires no porosity banding. The paper uses the Hyde field from the Southern North Sea as an example of the method. This dry gas field also has a Permian age, Rotliegendes reservoir comprised of an interbedded series of aeolian, fluvial and sabkha sediments. It has a broad

porosity range from 5-20% with a correspondingly wide permeability range of 0.1-10 mD and connate water saturation ranges from 25-50% depending on rock quality. While the method performs very well in the Southern North Sea gas fields on which it was founded, it may perform less well when large transition zones exist. Within a transition zone, the BVW-based relationship will break down.

**Capillary Pressure and Log-based Method (Skelt-Harrison & Skelt<sup>(8,9)</sup>).** Skelt recommends the fitting of a curve to a set of height and saturation data; initially to the capillary pressure data from SCAL, then refining this fit to the log derived water saturation data. Each data point can be assigned a different weight during the regression. This is useful if the analyst wants to characterise an extensive transition zone and applies a weighting factor based on the amount of gross rock area each data point "controls". The curve fitting routine minimises the sum of the absolute residual errors to remove the effect of outliers in the data set. The strength of Skelt's function is that, rather than linearise the function using logarithms, it makes use of its non-linearity to provide a fitted curve shape that actually looks like a capillary pressure curve. It works in the SCAL-based capillary pressure domain or the log-based water saturation domain. The equation takes the form:

$$S_w = 1 - A \cdot \exp\left[-\left(\frac{B}{(h+D)}\right)^C\right] \dots\dots\dots(10a)$$

where h is height above FWL and A, B, C and D are coefficients found by regression to core and log data.

The second form of the Skelt equation shown below is in Microsoft Excel format and **it works!** Please note that incorrect versions are given in the text of both of the previous papers by Skelt-Harrison, and Skelt.

$$SW = 1 - ((A)*EXP(-(((B)/(D + H))^C)) \dots\dots\dots(10b)$$

Be warned, depending on the version of Excel you are using, you do need to use **all** the brackets shown above.

Another feature of Skelt's method is that the coefficients "A, B, C and D" are functions of permeability that are found by the curve fitting procedure and H is height above FWL. Each of the constants allows us to shift the fitted capillary pressure curve in different ways. Coefficient "A" shifts the curve in the X-axis direction (i.e. the water saturation axis) and so allows a fit to the observed irreducible water saturation. Coefficient "B" shifts the curve in the Y-axis direction (i.e. the capillary pressure or height axis) and higher values of "B" even allow the threshold curvature to be modelled. Coefficient "C" is usually around a value of 1.0 and allows the elbow or inflexion of the capillary pressure curve to be matched. Coefficient "D" is simply a block shift to move the curve up and down to match an observed FWL. All the terms are found quite easily using an Excel spreadsheet. We have outlined the major elements of it below:

1. Set the coefficient "D" to zero as it is only used in the log matching process later.
2. Fit a curve, by altering the coefficients "A, B and C", to the capillary pressure measurements on each plug in turn.
3. This provides us with a table of values for the coefficients "A, B and C" for each core plug.
4. Set the value of coefficient "C" to its mean value (similar to Johnson), then refit the capillary pressure measurement data using the average value of constant "C" to derive a new set of constants "A and B".
5. Crossplot both of these new coefficients "A and B" against core plug permeability and derive relationships for both "A" and "B" as functions of permeability.
6. Convert from capillary pressure to height domain by applying a multiplier to the "B" permeability function in the Skelt equation.
7. Coefficient "D" can now be used, if needed, to move the fitted curve up and down the log-derived water saturation vs. depth until a best fit is obtained. This may be done by eye or regression.
8. If there is something awry, such as incorrect or insufficient SCAL data, we can match to the log-derived water saturation directly. Take the capillary pressure derived Skelt function and iterate on the "A and B" permeability functions to minimise errors between the Skelt function and the log derived water saturation curve.

Hence, Skelt's method can be used with either SCAL or log data. The matched capillary pressure shape can still be "pulled and stretched" to improve the fit to log data if need be.

### Comparative Analysis of the Saturation-Height Methods

Each of the saturation-height methods was used to predict saturation trends in our two example wells. Besides comparing the average saturation predicted in the well, we also determined the root mean squared (RMS) error in each case. This gives an idea of how faithfully the saturation-height functions predicted the example well saturation values.

The saturation trends were then integrated with associated gross rock area (GRA) vs. height curves to compute volumetric estimates of hydrocarbon in place. The example well data were also used to derive hydrocarbon in place estimates. These were then used to gauge how close the estimates from the saturation-height functions could get to the log-derived values.

**Water Saturation Differences.** The example log data from the UK North Sea are shown in Figures 1 and 2 for the oil well and gas well, respectively. The oil well was drilled with OBM and has had Dean Stark saturation measurements performed on its core. Thus, we were able to match our log-derived saturation values to them in the connate region. The transition zone begins where the log-derived saturation diverges from that of the Dean Stark measurements. Hence, we appear to have a transition zone of around 60 feet in the

example oil well. The oil saturation in the example well was, on average, 44%.

The gas well example does not have this luxury of Dean Stark saturation measurements, but we have obtained a good match on porosity. The Archie exponents are well documented for this basin, so we are reasonably confident in our log-derived saturation. The average gas saturation in the example well was 32%. The transition zone in this example gas well is still significant, possibly up to 45 feet (difficult to pin point exactly due to the changing facies through the well).

Figure 3 shows the results of the saturation-height fits to the oil well example. All of the functions do reasonably well at capturing the character of the saturation trend with height. As expected, the Cuddy function matched the lower oil saturation values very well indeed, but over-predicted the saturation in the lower poro-perm units nearer the FWL. At best, the saturation-height functions predicted observed oil saturation to within  $\pm 13\%$ . At worst, they predicted observed oil saturation to within  $\pm 25\%$ .

The Leverett fit, which relies on the capillary pressure measurement fitting a universal curve, is OK, but fails to match the high oil saturations in the better poro-perm sands in the top part of the well. This was found to be a banding problem, with the poorer poro-perm plugs exhibiting a different saturation relationship than those with higher poro-perm values. Figure 4 shows the extent of the problem and how much the Leverett coefficients can vary. The Leverett J-Function was re-run with a "binary switch" based on a trigger value of permeability of 20md, so the appropriate J-Function was used throughout the column. The resultant fit in Figure 5 shows a marked improvement in the saturation match in the upper sands. This is a workaround solution, but we then have the additional problem of having to predict poro-perm distribution accurately fieldwide in order to assign the appropriate saturation-height function.

Figure 6 shows the results of the saturation-height fits to the gas well example. All of the functions do well at capturing the character of the saturation trend with height. As expected, the Cuddy function, which was derived for use in this gas basin, matched gas saturation very well indeed. The Skelt function also performed very well. The two SCAL-based functions of Leverett and Johnson, being averaging techniques, struggled to match the dynamic character of the example well data. Overall however, the saturation-height functions predicted observed gas saturation very well to within  $\pm 8-13\%$ .

The results of all the saturation-height fits are shown in Table 2.

**Hydrocarbon-In-Place Differences.** The example GRA-height curves for the Palaeocene and Permian reservoir structures are shown in Figure 7. It can be seen that the transition zone volumes make up over half of the Palaeocene oil filled structure and about a third of the Permian gas filled structure. Hence, it is very important that the saturation-height function models the transition zone correctly, especially in the

oil case. The log-derived saturation was used to estimate hydrocarbon in place too. Use of log data predicted 378 Bscf for gas initially in place (GIIP) and 39.6 MMstb for stock tank oil in place (STOIP). These values served as a guide to how the saturation-height functions performed.

The GIIP estimates from the saturation-height functions were very tightly grouped and in close agreement with each other. In fact, they were only 2-4% more than estimated using log-derived saturation.

The STOIP estimates were more widely spread. In fact, we were surprised how close the estimates of the Leverett and Johnson methods were considering they had slightly worse fits to log-derived saturation. The volumetric equation appears to have cancelled out some of these errors to produce, on paper at least, a very good estimate of STOIP. But, maybe we shouldn't get too carried away as poro-perm banding will almost certainly be needed in a fieldwide exercise. Also, averaging saturation-height methods tend to predict the average saturation in a hydrocarbon column, rather than the actual value at a particular depth. We have already mentioned the Cuddy function's over prediction of oil saturation in the lower sands of the example well. This failing is compounded in the volumetric exercise as these sands "control" much larger rock volumes than the sands at the top of the column. Hence, the STOIP estimate from the Cuddy function is much higher than the others.

The results of all the hydrocarbon in place estimates from the different saturation-height functions are shown in Table 3.

## Conclusions

1. We have reviewed and compared the performance of four of the more popular saturation-height functions in use today. The methods of Leverett, Johnson, Cuddy and Skelt.
2. The methods were used to predict saturation-height in two UK North Sea data sets: a Palaeocene oil well and a Permian gas well. Each well had hydrocarbon columns in excess of 150 feet. The resulting saturation-height functions were then integrated with GRA-height transforms of typical North Sea reservoir structures to estimate volumetric hydrocarbon in place.
3. Cuddy's log-based method is the simplest and easiest to implement followed by Leverett's SCAL-based J-Function. The SCAL-based techniques of Johnson and Skelt are the most labour intensive for the analyst.
4. All of the methods on test performed reasonably well. Hydrocarbon saturation was predicted to within 13-25% in the oil well and to within 8-13% in the gas well.
5. The oil well SCAL data indicated two distinct poro-perm trends. This meant that the SCAL-based methods gave an average fit to the log data, showing less dynamic character (i.e. not matching the "peaks and troughs"). Using two poro-perm bands improved the match to log data. The drawback to banding is that we have to be able to predict the poro-perms accurately fieldwide in order to apply the correct saturation-height function.

6. All methods estimated GIIP very closely. Cuddy's function, which was derived for use in this gas basin, does particularly well. We conclude that any of the methods should perform well in gas fields.
7. There was a much larger spread in estimated STOIP. The Cuddy method over estimated STOIP due to the fact it uses a BVW approach (which breaks down in the transition zone) and has a preferential fit to the better quality rock. We conclude that the SCAL-based methods should perform better in oil fields. This is especially true in low relief structures where the transition zone is a major part of the reservoir.

## Nomenclature

$g$  = acceleration due to gravity, m/sec/sec

$h$  = height above free water level, ft

$J$  = Leverett function, dimensionless

$K$  = permeability, md

$P_c$  = capillary pressure, psi

$r$  = pore radius, cm

$S_w$  = water saturation

$S_{wirr}$  = irreducible water saturation

$\phi$  = porosity interfacial tension, dynes/cm<sup>2</sup>

$\theta$  = contact angle, degrees

$\rho_o$  = oil density, g/cm<sup>3</sup>

$\rho_w$  = water density, g/cm<sup>3</sup>

$\sigma$  = interfacial tension, dynes/cm<sup>2</sup>

## Acknowledgements

We thank the London Petrophysical Society (LPS) for making the data available.

## References

1. Amyx, J.W., Bass, D.M. Jr. and Whiting, R.L.: "Petroleum reservoir engineering" McGraw-Hill Book Company (1960).
2. Wall, C.G., Archer, J.S.: "Petroleum engineering principles and practice", Graham & Trotman Ltd. (1986).
3. Core Laboratories: "Special core analysis". Dallas, (1982).
4. Adamson, A.W.: "Physical chemistry of surfaces", Wiley, New York, (1976).
5. Leverett, M.C.: "Capillary behaviour in porous solids" Petroleum Transactions of AIME 142 (1941) pp 152-169.
6. Johnson, A.: "Permeability averaged capillary data: a supplement to log analysis in field studies", Paper EE, SPWLA 28<sup>th</sup> Annual Logging Symposium, June 29<sup>th</sup> - July 2<sup>nd</sup> (1987).
7. Cuddy, S., Allinson, G. and Steele, R.: "A simple, convincing model for calculating water saturations in Southern North Sea gas fields", Paper H, SPWLA 34<sup>th</sup> Annual Logging Symposium, June 13<sup>th</sup> - 16<sup>th</sup> (1993).
8. Skelt, C. and Harrison, R.: "An integrated approach to saturation height analysis", Paper NNN, SPWLA 36<sup>th</sup> Annual Logging Symposium, (1995).
9. Skelt, C.: "A relationship between height, saturation, permeability and porosity", Paper E018, 17<sup>th</sup> European Formation evaluation Symposium (SPWLA), Amsterdam, 3-7 June (1996).

**Table 1: Interfacial Tension & Contact Angle Values (Core Laboratories, 1982)**

Wetting-phase	Non-wetting phase	Conditions T = temperature P = pressure	Contact Angle $\theta$	IFT(dynes/cm) $\sigma$
Brine	Oil	Reservoir T,P	30	30
Brine	Oil	Laboratory T,P	30	48
Brine	Gas	Laboratory T,P	0	72
Brine	Gas	Reservoir T,P	0	50
Oil	Gas	Reservoir T,P	0	4
Gas	Mercury	Laboratory T,P	140	480

**Table 2: Saturation Results.**

UK SNS Gas Well Example:

	Example Well	Leverett	Johnson	Cuddy	Skelt
Average Sg	32%	32%	31%	30%	32%
RMS error in Sg	0	± 11%	± 13%	± 10%	± 8%

UK CNS Oil Well Example:

	Example Well	Leverett	Johnson	Cuddy	Skelt
Average So	44%	44%	40%	51%	38%
RMS error in So	0	± 18%	± 19%	± 25%	± 13%

**Table 3: Hydrocarbon-in-Place Results.**

UK SNS Gas Well Example:

	Example Well	Leverett	Johnson	Cuddy	Skelt
GIIP (Bscf)	378	385	389	394	385
GIIP difference	0	+ 2%	+3%	+4%	+2%

UK CNS Oil Well Example:

	Example Well	Leverett	Johnson	Cuddy	Skelt
STOIIP (MMb)	39.6	40.0	39.6	48.5	34.3
STOIIP difference	0	+ 1%	0%	+23%	-13%

Figure 1 : UK CNS Oil Well Example - Log & Core Data

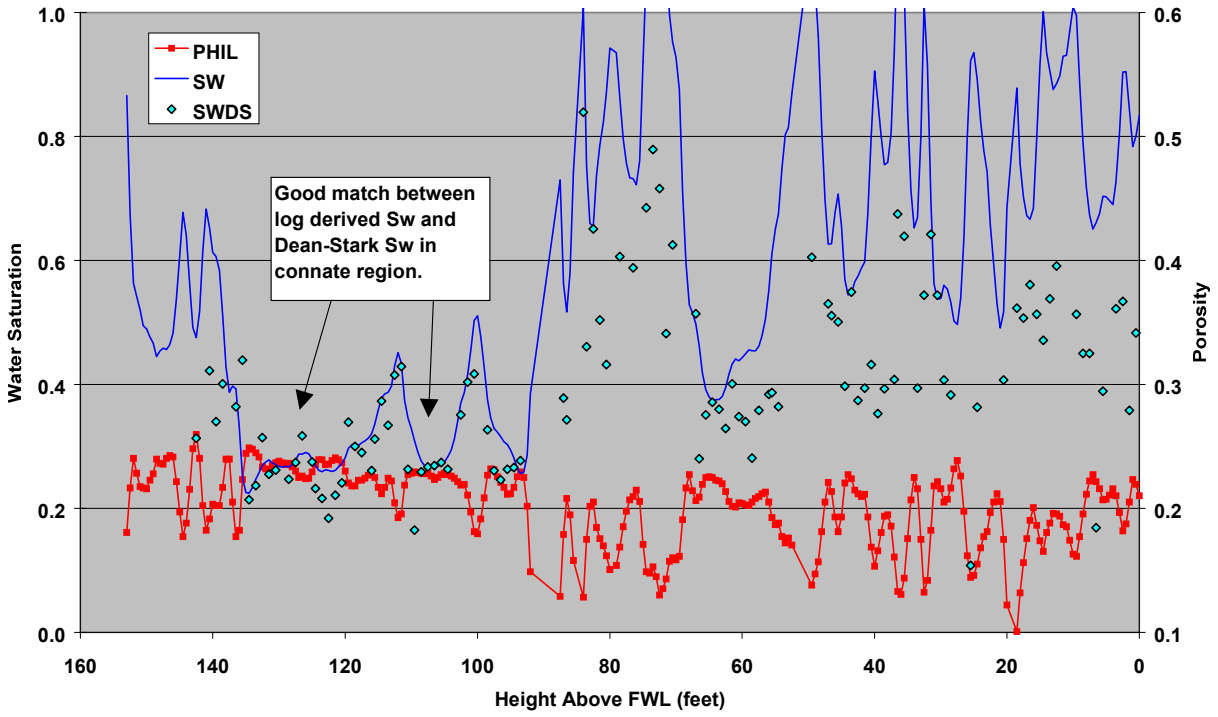
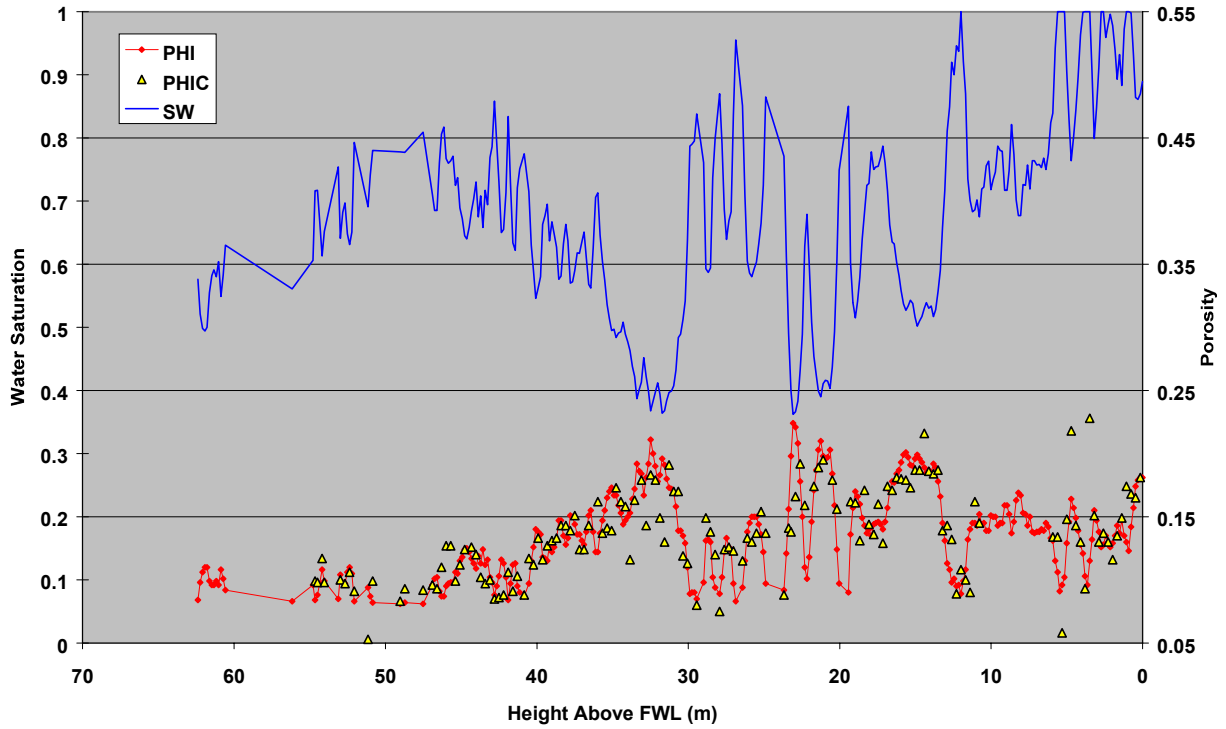


Figure 2 : UK SNS Gas Well Example - Log & Core Data



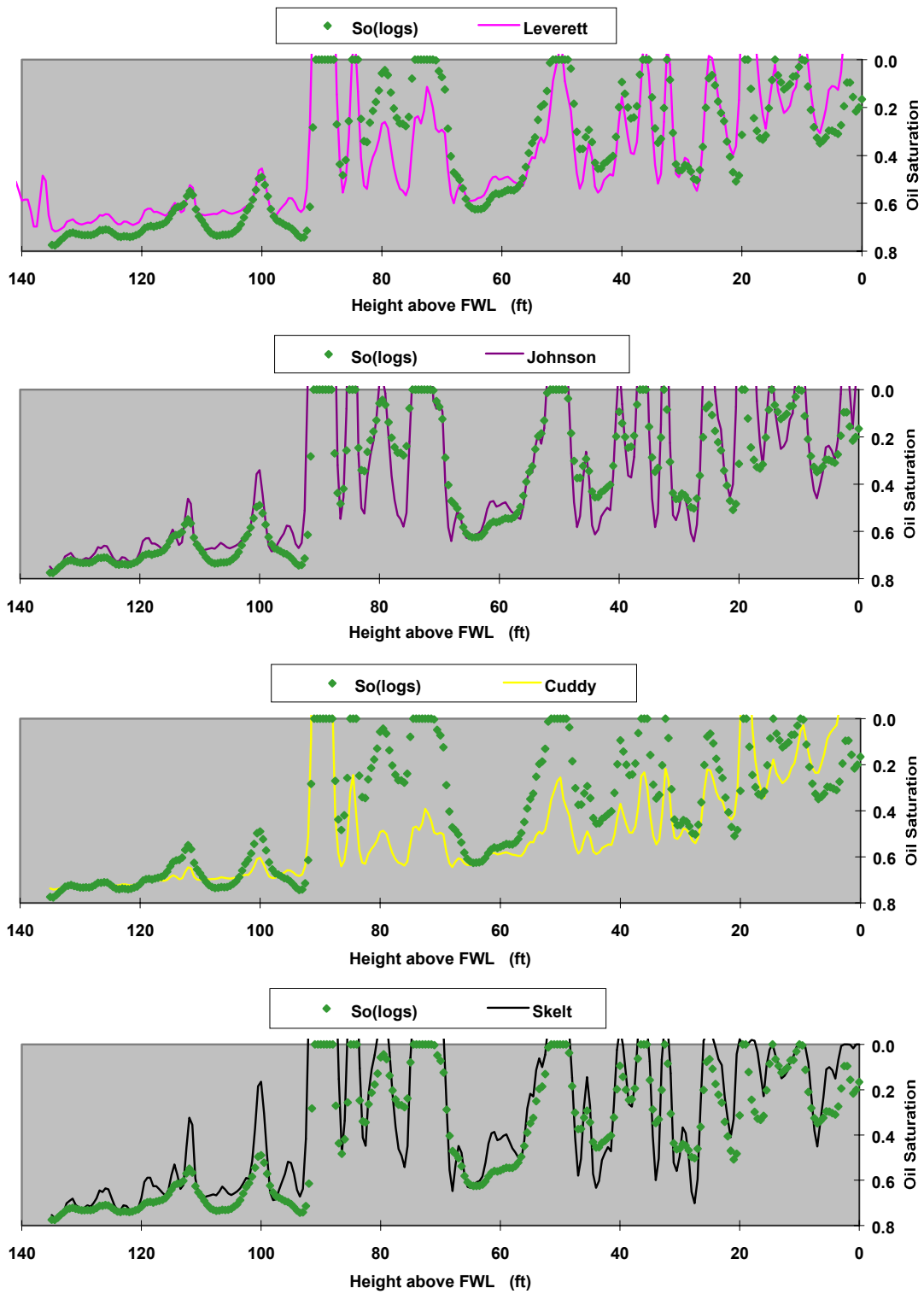
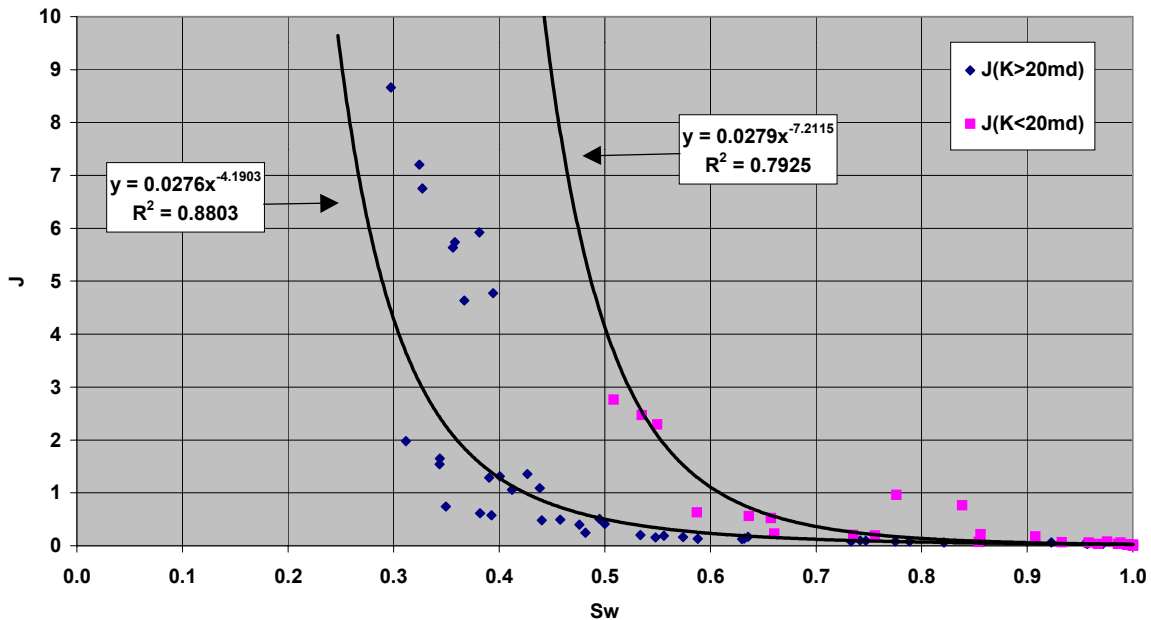
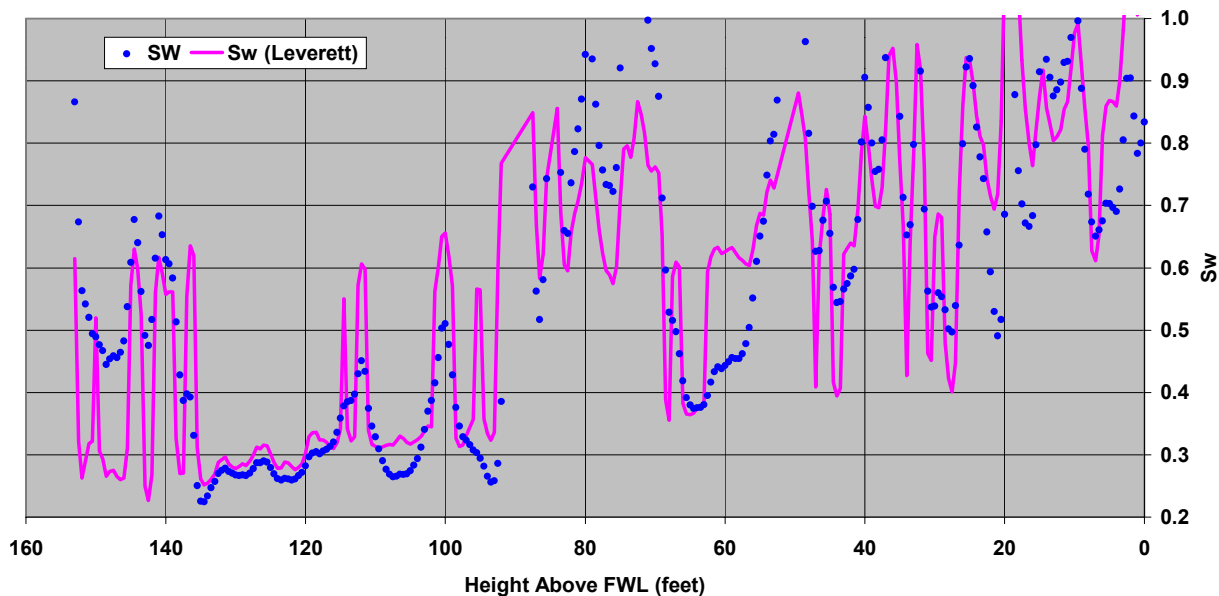


Figure 3: Saturation-Height Functions for UK CNS Oil Well Example

**Figure 4: Two Leverett J-Functions After Banding of SCAL Data (UK CNS Oil Well Example)**



**Figure 5: Better Sw Match with Improved Leverett J-Function from SCAL Data Banding (UK CNS OIL Well Example)**



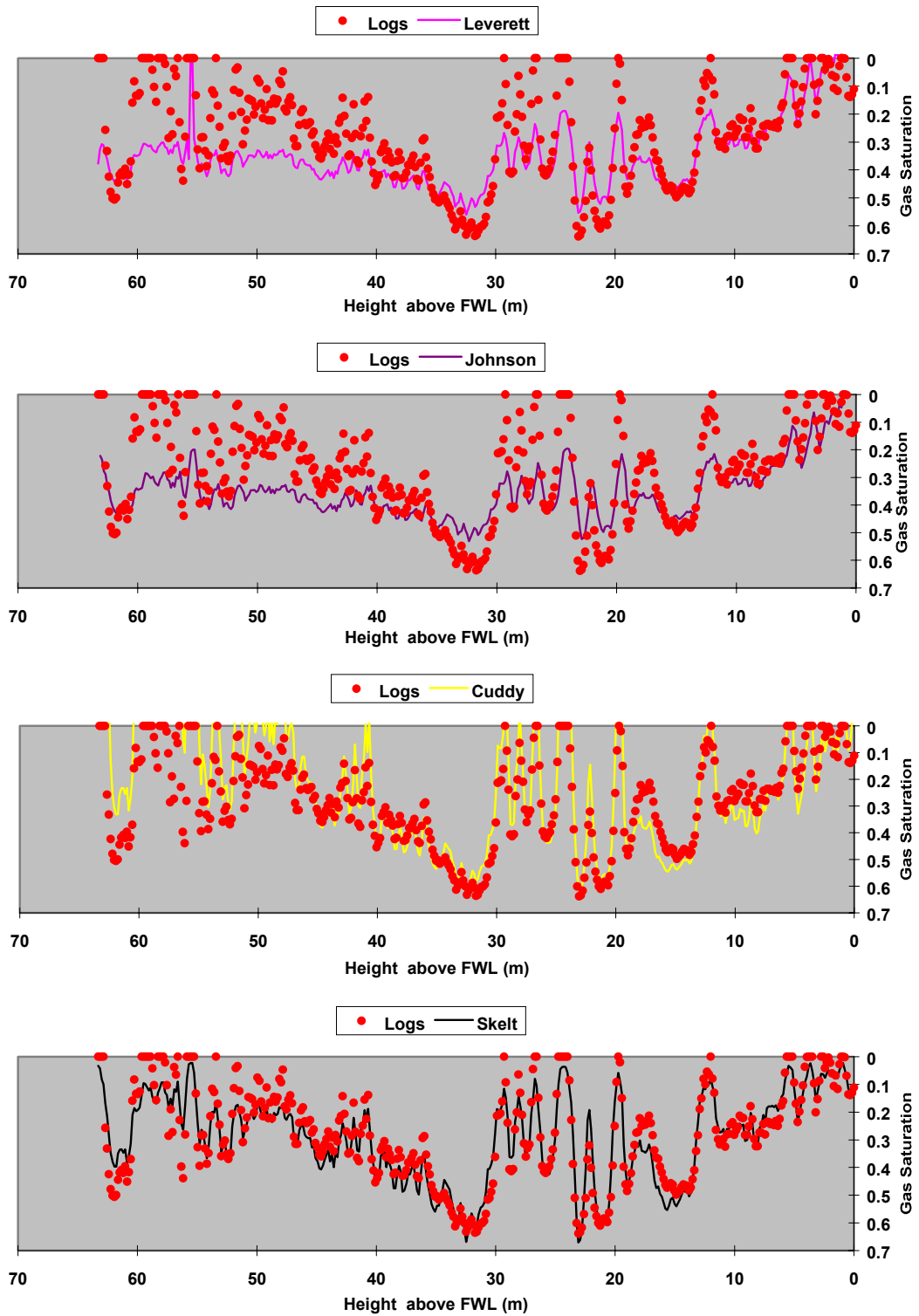


Figure 6: Saturation-Height Functions for UK SNS Gas Well Example

**Figure 7: Comparison of Reservoir Areas vs. Height above Free Water Level for North Sea Well Examples**

